



Astrophysics and cosmology with galaxy clusters: the WFXT perspective

S. Borgani^{1,2,3}, P. Rosati⁴, B. Sartoris^{1,2,3}, P. Tozzi^{2,3}, R. Giacconi⁵, & the WFXT Team

¹ Dipartimento di Fisica, Sezione di Astronomia, Università di Trieste, Via Tiepolo 11, I-34143 Trieste, Italy e-mail: borgani, sartoris@oats.inaf.it

² INAF-Osservatorio Astronomico di Trieste, Via Tiepolo 11, I-34143 Trieste, Italy e-mail: tozzi@oats.inaf.it

³ INFN, Sezione di Trieste, Via Valerio 2, I-34127 Trieste, Italy

⁴ ESO-European Southern Observatory, D-85748 Garching bei München, Germany e-mail: prosati@eso.org

⁵ Department of Physics and Astronomy, The Johns Hopkins University, Baltimore MD, USA

Abstract. We discuss the central role played by the X-ray study of galaxy clusters to reconstruct the assembly of cosmic structures. We shortly review the progress in this field contributed by the current generation of X-ray telescopes. Then, we focus on the outstanding scientific questions that have been opened by observations carried out in the last years by Chandra and XMM: (a) When and how is entropy injected into the inter-galactic medium (IGM)? (b) What is the history of metal enrichment of the IGM? (c) What physical mechanisms determine the presence of cool cores in galaxy clusters? (d) How is the appearance of proto-clusters at $z \geq 2$ related to the peak of star formation activity and BH accretion? (e) What do galaxy clusters tell us about the nature of primordial density perturbations and on the history of their growth? We argue that the most efficient observational strategy to address these questions is to carry out a large-area X-ray survey, reaching a sensitivity comparable to that of deep Chandra and XMM pointings, but extending over several thousands of square degrees. A similar survey can only be carried out with a Wide-Field X-ray Telescope (WFXT), which combines a high survey speed with a sharp PSF across the entire FoV.

Key words. Cosmology – galaxy clusters – X-rays

1. Introduction

Galaxy clusters represent the place where astrophysics and cosmology meet: while their overall internal dynamics is dominated by gravity, the astrophysical processes taking place on galactic scale leave observable imprints on the diffuse hot gas trapped within their potential wells (Rosati et al.

2002; Voit 2005; Borgani & Kravtsov 2009). Understanding in detail the relative role played by different astrophysical phenomena in determining this cosmic cycle of baryons, and its relationship with the process of galaxy formation, is one of the most important challenges of modern cosmology. Clusters of galaxies represent the end result of the collapse of density

fluctuations over comoving scales of about 10 Mpc. For this reason, they mark the transition between two distinct dynamical regimes. On scales roughly above 10 Mpc, the evolution of the structure of the universe is mainly driven by gravity and the evolution still feels the imprint of the cosmological initial conditions. At scales below 1 Mpc the physics of baryons plays an important role in addition to gravity, thus making physical modeling far more complex. In the current paradigm of structure formation, clusters form via a hierarchical sequence of gravitational mergers and accretion of smaller systems. Within these small halos gas efficiently cools, forms stars and accretes onto supermassive black holes (SMBHs), living in massive galaxies, already at high redshift. While the star formation peaks at redshift $z \sim 2-3$, the intergalactic gas is heated to high, X-ray emitting temperatures by adiabatic compression and shocks, and settles in hydrostatic equilibrium within the cluster potential well, only at relatively low redshift, $z \lesssim 2$. The process of cooling and formation of stars and SMBHs can then result in energetic feedback due to supernovae or AGN, which inject substantial amounts of heat into the intergalactic medium (IGM) and spread heavy elements throughout the forming clusters.

Galaxy clusters are also very powerful cosmological tools. They probe the high end of the mass function of dark matter (DM) halos, whose evolution is highly sensitive to the underlying cosmological scenario and to the growth rate of cosmological perturbations (e.g., Borgani et al. 2001; Voit 2005). This information, combined with the shape and amplitude of the power spectrum of their large-scale distribution, offers a means of constraining the growth of cosmic structures over a wide range of scales. For these reasons, galaxy clusters are nowadays considered sensitive probes of the dark sector of the Universe and of the nature of gravity, complementary to CMB and SN-Ia tests, which are sensitive to the background geometry and expansion rate. Based on relatively small samples of few tens of distant X-ray clusters extracted from ROSAT deep pointings, followed up by Chandra observations, independent analyses have recently shown that the

evolution of the population of galaxy clusters does indeed provide significant constraints on cosmological parameters (e.g. Vikhlinin et al. 2009a; Mantz et al. 2009). This remarkable progress in cluster cosmology has been made possible by the introduction of robust X-ray mass proxies, such as the gas mass M_{gas} and the total thermal content of the ICM defined by the product of gas mass and temperature, $Y_X = M_{gas}T$ (e.g. Kravtsov et al. 2006). Quite interestingly, the scatter in the relation between such mass proxies and the total cluster mass is suppressed after excising core cluster regions, $\lesssim 0.15R_{500}$.

Such results demonstrate that, to fully exploit the potential of clusters for cosmological applications, detailed measurements of X-ray mass requires collecting an adequate number of photons and good spatial resolution to remove the contribution of core regions in distant objects. From one hand, the revitalization of cluster cosmology has indeed required the high data quality offered by the present generation of X-ray satellites. On the other hand, it highlights the constraining power that future X-ray surveys, like the one to be provided WFXT, could provide. The WFXT surveys would increase by several orders of magnitude the statistics of distant clusters for which data of comparable quality as that provided by Chandra observation.

As we will discuss in this contribution, the large grasp of WFXT combined with its sharp and stable PSF makes it the ideal instrument for astrophysical and cosmological studies of galaxy clusters (see also Giacconi et al. 2009, Vikhlinin et al. 2009b, and Rosati et al., in this volume).

2. WFXT to study clusters as astrophysical laboratories

Thanks to the high density and temperature reached by the gas within their potential wells, galaxy clusters mark the only regions where thermo- and chemo-dynamical properties of the IGM can be studied in detail at $z < 1$ from X-ray emission, and directly connected to the optical/near-IR properties of the galaxy population. A remarkable leap forward in the

quality of X-ray observations of clusters took place with the advent of the Chandra and XMM-Newton satellites. Thanks to their unprecedented sensitivity (and angular resolution in case of Chandra), they led to a number of fundamental discoveries concerning nearby, $z \lesssim 0.3$, clusters. For instance:

- The lack of strong emission lines at soft X-ray energies in the core regions placed strong limits on the amount of gas that can cool to low temperatures (Peterson & Fabian 2006), thus challenging the classical cooling flow model (Fabian 1994);
- Temperature profiles have been unambiguously observed to decline outside the core regions and out to the largest radii sampled so far, $\sim R_{500}^1$, while they gently decline toward the cluster center in relaxed systems (e.g. Vikhlinin et al. 2005; Pratt et al. 2007; Leccardi & Molendi 2008b);
- The level of gas entropy at R_{500} is in excess of what explainable by the action of supersonic accretion shocks (e.g. Sun et al. 2009; Pratt et al. 2009), while it is unexpectedly low in the innermost regions of relaxed clusters (e.g. Donahue et al. 2006);
- The intra-cluster medium (ICM) is not uniformly enriched in metals, instead metallicity profiles are observed to have a spike in the central regions, associated to the presence of the brightest cluster galaxy (BCG), while declining at least out to $\approx 0.3R_{500}$.

While these observations shed new light on our understanding of the physical properties of the low-redshift intergalactic medium, (IGM), they opened at the same time at least as many questions. As we will discuss here below, an efficient way of addressing open questions in the ICM study is by carrying out high-sensitivity X-ray surveys, which provide a large number of clusters for which detailed

¹ We indicate with R_Δ the cluster-centric radius encompassing an average overdensity Δ times the critical cosmic density. For reference, $\Delta = 200$ is close to the virial overdensity while $\Delta = 500$ corresponds to about half the virial radius for a concordance Λ CDM model.

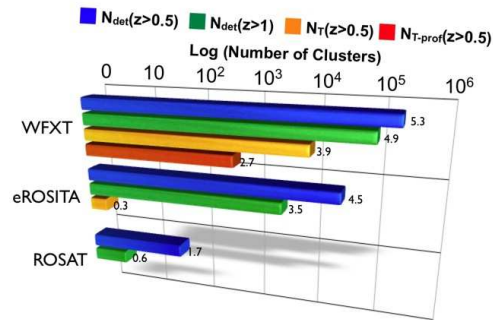


Fig. 1. The comparison between numbers of clusters expected for the surveys to be carried out by WFXT (as described in the contribution by Rosati et al. in this volume), by eROSITA, and as found in the ROSAT All Sky Survey (Voges et al. 1999). Blue and green bars: number of clusters detected at $z > 0.5$ and $z > 1$, respectively; yellow and orange bars: number of clusters with at least 1.5×10^3 and 1.5×10^4 net photon counts in the [0.5–2] keV energy band, respectively.

studies can be carried out at low and high redshift. In Figure 1, we show a comparison for the yields of clusters expected from five years of operation of WFXT, compared with the expectations for the planned German-led mission eROSITA². Besides the huge number of clusters that WFXT will detect at large redshift, this demonstrates that measurements of the physical properties of the ICM will be available for a large number of them.

When and how is entropy injected into the IGM? The standard explanation for the excess of entropy observed out to R_{500} is that some energetic phenomena should have heated the ICM over the cluster life-time (e.g. Voit 2005; Borgani & Kravtsov 2009). Models based on the so-called pre-heating (i.e. diffuse entropy injection before the bulk of the mass is accreted into the cluster halos) have been proposed as an explanation (e.g. Tozzi & Norman 2001; Borgani et al. 2002; Voit et al. 2003). However, these models predict quite large isentropic cores, which are not observed. Furthermore,

² Based on the specifications as provided in Mission Definition Document (<http://www.mpe.mpg.de/erosita/MDD-6.pdf>)

studies of the intergalactic medium (IGM), from observations of $z \gtrsim 2$ absorption systems in high-resolution optical spectra of distant QSOs, demonstrate that any pre-heating should take place only in high-density regions (Shang et al. 2007; Borgani & Viel 2009). An alternative scenario is that ICM heating takes place at relatively low redshift, within an already assembled deep potential well. In this case, the natural expectation is that the same heating agent, presumably the central AGN, should be responsible for both establishing the cool core and increasing the entropy out to ~ 1 Mpc scale, although it is not clear how AGN feedback can be distributed within such a large portion of the cluster volume.

Reconstructing the timing and pattern of entropy injection in the ICM has far reaching implications for tracing the past history of star formation and black hole (BH) accretion. While we expect that the two above scenarios leave distinct signatures on the evolution of the ICM entropy structure, available data from XMM and Chandra are too sparse to adequately understand this evolution.

The large number of clusters with $\sim 10^4$ counts available from the WFXT surveys would increase by orders of magnitude the statistics of a handful of clusters at $z > 0.5$ for which detailed entropy profiles have been measured so far. The measurement of ICM profiles for a large number of distant clusters will allow us to trace the interplay between IGM and galaxy population along 2/3 of the cosmological past light-cone. Furthermore, the low background and the possibility of resolving out the contribution of point sources will also allow us to measure such profiles out to R_{200} and beyond for bright galaxy clusters at $z < 0.2$ (see the contribution by Ettori & Molendi, in this volume).

What is the history of metal enrichment of the IGM? This question is inextricably linked to the previous one on the history of IGM heating. Measurements of the metal content of the ICM provide direct information on the past history of star formation and on processes (e.g., galactic ejecta powered by SN and AGN, ram-pressure stripping of merging galaxies, stochastic gas motions, etc.) that are expected

to displace metal-enriched gas from star forming regions (e.g., Schindler & Diaferio 2008). So far, X-ray observations have provided valuable information on the pattern of enrichment only at low-redshift, $z \lesssim 0.3$ (Baumgartner et al. 2005; Mushotzky 2004; Werner et al. 2006). Profiles of the Fe abundance have been measured for nearby systems (e.g. Snowden et al. 2008; Leccardi & Molendi 2008a). However, these results are limited to rather small radii, $\lesssim 0.3R_{500}$, while the level of enrichment at larger radii should be quite sensitive to the timing of metal production and to the mechanism of metal transport. Furthermore, profiles of chemical abundances for other elements, such as O, Si, and Mg, are much more uncertain. Tracing the relative abundances of different chemical species, which are synthesized in different proportions by different stellar populations, is crucial to infer the relative role played by different SN types and to establish the time-scale over which the ICM enrichment took place. The situation is even more uncertain at $z > 0.3$. Although analyses based (mainly) on the Chandra archive show indications for an increase of the ICM enrichment since $z \sim 1$ (Balestra et al. 2007; Maughan et al. 2008), basically no information is available on the metallicity profiles and on abundance of elements other than Fe. To improve upon this situation, one needs (a) to push to larger radii the study of the distribution in the ICM of different chemical species in nearby clusters; (b) to measure profiles of the Fe abundance for hundreds of clusters at $z > 0.5$.

Iron metallicity profiles would be measured by WFXT for virtually all the clusters for which a temperature profile is obtained, although with ~ 2 times larger statistical errors. A very accurate measurement of the global Fe metallicity will be obtained for several thousands of clusters out to $z \sim 1.5$. For all the clusters of this sample, thermo-dynamical and chemical properties of the ICM will be characterized with unprecedented precision.

What physical mechanisms determine the presence of cool cores in galaxy clusters? XMM and Chandra unambiguously demonstrated that the rate of gas cooling in cluster cores is unexpectedly low. Such a low cooling

rate requires that some sort of energy feedback must heat the ICM so as to exactly balance radiative losses. AGN are generally considered as the natural solution to this problem (e.g. McNamara & Nulsen 2007). However, no consensus has been reached so far on the relative role played by AGN and by mergers in determining the occurrence of cool cores in galaxy clusters (e.g. Burns et al. 2008). Since merging activity and galactic nuclear activity are both expected to evolve with redshift, measurements of the occurrence of cool cores in distant clusters are necessary to address this issue. Although attempts have been pursued to characterize the evolution of the fraction of cool cores using Chandra data (e.g. Santos et al. 2008), no definite conclusion has been reached on the evolution of the fraction of cool core clusters.

The sharp and stable PSF of WFXT will allow one to resolve the core region of distant clusters (a cool-core of 50 kpc radius will subtend an angle of ≈ 6 arcsec at $z = 1$). The yield of hundreds of clusters at $z > 0.5$ for which more than 10^4 counts will be available, will allow us to accurately measure the evolution of the occurrence of cool cores and how this is related to the cluster dynamical state.

How is the appearance of proto-clusters related to the peak of star formation activity and BH accretion? Massive galaxies in today's clusters show only very modest ongoing star formation: they harbor a super-massive black hole usually living in a quiescent accretion mode and experience only “dry” mergers with much smaller galaxies. The situation should be radically different at $z \sim 2$. This is the epoch when proto-BCGs are expected to be assembling through violent mergers between actively star-bursting galaxies, moving within a rapidly evolving potential well. These proto-cluster regions accrete a large amount of gas that is suddenly heated to high temperature by mechanical shocks and, for the first time, starts radiating in X-rays. At the same time, BHs hosted within merging galaxies are expected to coalesce and their accretion disks to be destabilized by the intense dynamical activity, thereby triggering a powerful release of feedback energy. Evidence for such forming proto-

clusters has been obtained by optical observations of a strong galaxy overdensity region, the so-called Spiderweb complex, surrounding a previously identified powerful radio galaxy at $z \approx 2.1$ (Miley et al. 2006; Hatch et al. 2009). Cosmological simulations lend support to the expectation that similar structures trace the progenitors of massive cluster seen locally, and predict that this structure should already contain dense IGM, emitting in X-rays with $L_X \sim 10^{44}$ erg s $^{-1}$ in the [0.5-2] keV band, with a temperature of several keV and enriched in metal at a level comparable to nearby clusters (Saro et al. 2009). As of today, no unambiguous detection of X-ray emitting gas permeating this region has been obtained (Carilli et al. 2002). While the detection of such a hot diffuse gas may be just at the limit of the capability of current X-ray telescopes, characterizing its physical properties (temperature and metallicity) is far beyond the reach of Chandra and XMM.

The study of proto-clusters at $z \gtrsim 2$ is still unexplored territory. For this reason, it is difficult to make predictions on how many of these structures could be observed by WFXT. By extrapolating our present knowledge of the relation between mass and X-ray luminosity, we expect to detect several hundreds of such objects over the whole sky. For the brightest of these clusters, it will even be possible to measure their redshift through X-ray spectroscopy with deeper follow-up exposures. At $z \sim 2$ the inverse Compton scattering of relativistic electrons, injected by AGN in core regions, off the CMB photons is much more effective than at low- z in producing a hard X-ray excess, thanks to the higher CMB temperature. Based on the expectation from hydrodynamic simulations, we estimated that 5 to 10 thousands of photons would be detectable by WFXT in a deep 400 ksec pointing on a $z \approx 2$ proto-cluster, which is the progenitor of a today massive cluster, with $M_{200} \approx 10^{15} h^{-1} M_\odot$. Such an observation would allow one: (a) to catch “in fieri” the pristine ICM enrichment; (b) to see in action the combined effect of strong mergers and intense nuclear activity within a forming cluster; (c) to discern the thermal and non-thermal emission from X-ray spectroscopy and infer the early

contribution of cosmic rays in pressurizing the ICM.

The goal of measuring physical properties of the ICM out to $z \sim 1$ and beyond can only be accomplished by a survey with the area and sensitivity achievable with WFXT. In fact, WFXT constitutes a two orders of magnitude improvement with respect to eROSITA (similar to the area-sensitivity enhancement that eROSITA will give with respect to the ROSAT All-Sky Survey), with in addition a 5 times better angular resolution (see the contribution by Cappelluti et al, in this volume).

3. Cluster cosmology with WFXT

WFXT will not be just a highly efficient cluster-counting machine. Its unique added value is that it will characterize the physical properties for a good fraction of these clusters and, therefore, calibrate them as robust tools for cosmological applications. Based on the specification of the WFXT surveys (see Rosati et al., this volume), we computed the constraints that can be placed on different classes of cosmological models. By following the approach described by Sartoris et al. (2010), we apply the Fisher-Matrix technique to forecast constraints on cosmology by combining information from number counts and power spectrum of clusters. The computation of these forecasts is based on the so-called self-calibration approach (e.g., Majumdar & Mohr 2003; Lima & Hu 2004). In this approach, we assume that X-ray observations provide an estimate of the actual cluster mass whose uncertain relation with the actual cluster mass is described by a suitable set of ‘nuisance’ parameters, to be fitted, with their own priors, along with cosmological parameters.

Sartoris et al. (2010) used this approach to place constraints on possible deviations from Gaussianity of the primordial density fluctuation field. The reference cosmological model assumed in this analysis, consistent with the WMAP-7 best-fitting model (Komatsu et al. 2010), assume: $\Omega_m = 0.28$, $\sigma_8 = 0.81$, $\Omega_k = 0$ for the curvature, $w(a) = w_0 + (1 - a) w_a$ with $w_0 = -0.99$ and $w_a = 0$ for the Dark Energy

equation of state, $\Omega_b = 0.046$ for the baryon contribution, $h = 0.70$ for the Hubble parameter, $n = 0.96$ for the primordial spectral index and $f_{NL} = 0$ for the non-Gaussianity parameter. Furthermore, in the analysis we also include priors on cosmological parameters as expected from the Planck CMB experiment (Rassat et al. 2008).

We adopt the appropriate flux-dependent sky coverages for the three surveys (see Tozzi et al., this volume). To convert fluxes into masses, we use the relation between X-ray luminosity and M_{500} calibrated by Maughan (2007), where masses are recovered from Y_X , using Chandra data for 115 clusters in the redshift range $0.1 < z < 1.3$. The relation between measured and true mass is described by four nuisance parameters, which describe a possible intrinsic bias in the mass estimate, e.g. related to a residual violation of hydrostatic equilibrium (e.g. Rasia et al. 2006; Piffaretti & Valdarnini 2008; Lau et al. 2009), an intrinsic scatter in this relation and the evolution of these two parameters (see Sartoris et al. 2010, for a more detailed discussion).

In the left panel of Figure 2 we show the redshift distribution for all the clusters detected in the three WFXT surveys, having mass of at least $M_{500} > 5 \times 10^{13} h^{-1} M_\odot$. The right panel shows the same redshift distributions for the ‘Golden Samples’, i.e. for all the clusters which are detected with at least 1500 net photon counts. The left panel demonstrates the huge potential of WFXT to detect a large number of clusters out to $z \sim 2$ and beyond. Furthermore, the right panel demonstrates that WFXT is not only a highly efficient survey machine to count clusters. In fact, its large grasp also provides a large enough number of photons and, therefore, to precise measurements of robust mass proxies, for about 20,000 clusters, with ~ 1000 of them at $z > 1$. This represents a huge improvement with respect to the few tens of distant clusters available at present. This plot also shows the relevance of the Deep Survey to calibrate measurements of mass proxies beyond $z \sim 1$, thus complementing the larger statistics of lower- z clusters provided by the Medium and Wide surveys.

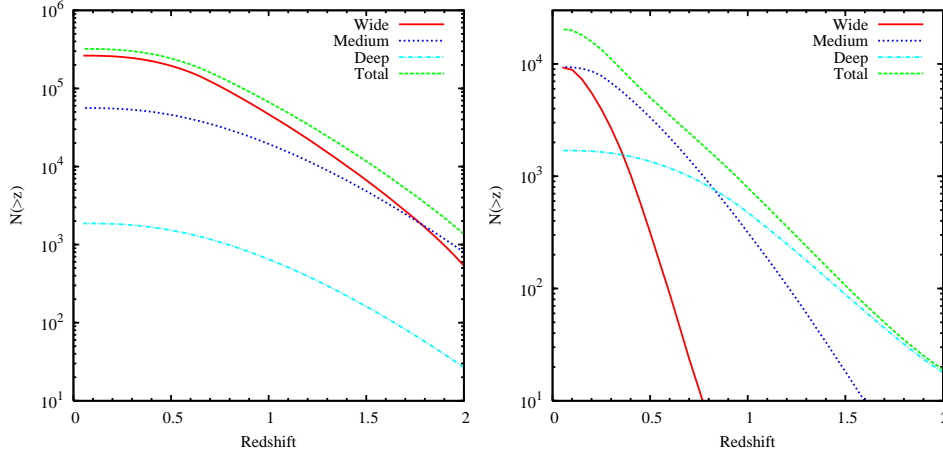


Fig. 2. The cumulative redshift distributions for the three WFXT surveys. The left panel is for all clusters detected, while the right panel is for the clusters in the “Golden Samples”, corresponding to a 1500 photons detected. In both panels solid (red), dotted (blue) and dot-dashed (cyan) curves are for the Wide, Medium and Deep surveys, respectively, while the short-dashed (green) curve is for the sum of the three surveys.

We show in Figure 3 the joint constraints on the f_{NL} parameter, which define the deviation from Gaussianity (e.g. Verde 2010; Desjacques & Seljak 2010, for recent reviews) and the normalization of the power spectrum, σ_8 , after marginalizing over all the other cosmological and nuisance parameters. As discussed by Sartoris et al. (2010) (see also Oguri 2009; Cunha et al. 2010), constraints on non-Gaussianity are weakly sensitive to the uncertain knowledge of the nuisance parameters. On the other hand, non-Gaussian constraints mainly comes from the shape of the power spectrum at the long wavelengths probing the possible scale dependence of the biasing parameter. For these reasons, we used in this analysis the large sets of detected clusters, without restricting to the “Golden Sample” for which nuisance parameters can be measured. This plot clearly shows that most of the constraints on non-Gaussianity comes from the Wide survey, which in fact has the potential to probe the long wavelength modes. Little information is carried instead by the Deep survey, which is instead very important for the calibration of mass proxies for distant clusters.

Figure 4 shows the constraints on the parameters defining the DE equation of state us-

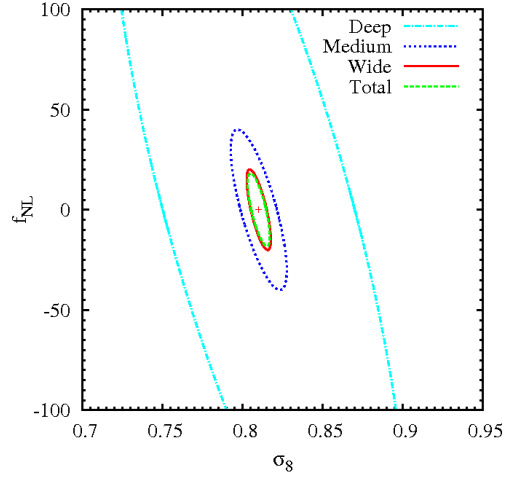


Fig. 3. Constraints at the 68 per cent confidence level on non-Gaussian parameter f_{NL} and power spectrum normalization σ_8 from the Deep, Medium and Wide surveys (solid red, long-dashed blue and short-dashed black curves, respectively), by combining number counts and power spectrum information. Also shown with the dotted magenta curve are the constraints obtained from the combination of the three surveys. No prior knowledge is assumed for the values of the nuisance parameters. The Fisher Matrix from Planck experiment is included in the calculation of all constraints.

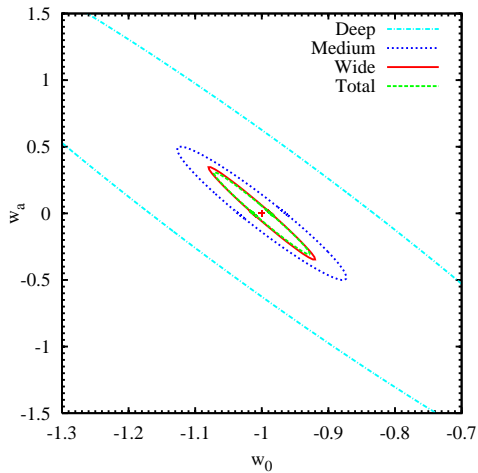


Fig. 4. The same as in Fig. 3, but for the constraints on the DE equation of state. The analysis is carried out for the same samples and same priors on nuisance parameters as in Fig.3.

ing the samples and the same priors on nuisance parameters as for Fig.3. Also in this case, the large cluster statistics available in the Wide survey, makes it providing the dominant constraining power. The resulting value of the DETF Figure-of-Merit Albrecht et al. (2009), after combining the information from the three surveys, is $DETF = 512$.

Figure 5 emphasizes the improvement represented by WFXT with respect to present constraints from X-ray cluster surveys. In this plot, the red shaded area show the constraints on the $\Omega_{DE}-w_0$ plane obtained by Vikhlinin et al. (2009a) from a sample combining nearby and distant cluster, originally identified from ROSAT data and followed-up with Chandra. Since Chandra follow-up provides at least $\sim 10^3$ photons per cluster, for consistency we compare it with the forecasts for the WFXT samples (light blue ellipse). The WFXT contour, which is obtained by combining number counts and power spectrum information, is off-centered with respect to the contours by Vikhlinin et al. (2009a) since their best-fitting model does not coincide with the reference cosmological model assumed for our Fisher-Matrix analysis of forecasts.

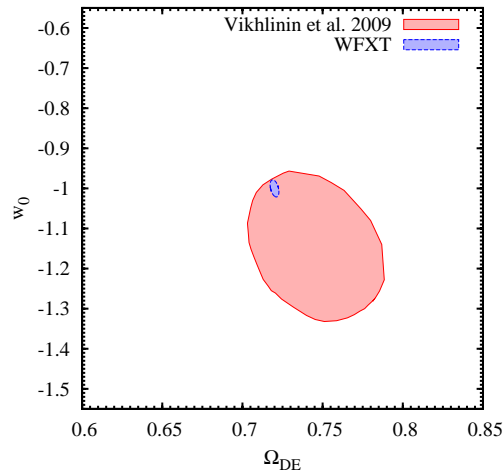


Fig. 5. A comparison between the constraints on the $\Omega_{DE}-w_0$ plane obtained by Vikhlinin et al. (2009a) from a sample of clusters followed-up with Chandra (red shaded area), and as expected for the “Bright” WFXT surveys, by combining number counts and power spectrum information, under the assumption of strong strong priors on the nuisance parameters (light blue filled area). Both contours corresponds to $\Delta\chi^2 = 1$ (i.e. 68 per cent confidence level for one significant parameter) and are obtained under the assumption of flat Universe.

As well known, the evolution of the population of galaxy clusters is affected by cosmology both through the cosmic expansion history, which defines the volumes, and through the linear growth rate of perturbations (e.g. Haiman et al. 2001). In order to make a pure test of perturbation growth, we decided to carry out the Fisher-Matrix analysis by freezing the expansion history to the Λ CDM one, while using a suitable parametrization to describe the growth history. A commonly adopted approach to parametrize the growth of perturbations is based on the quantity

$$f(a) = \frac{d \log D_+(a)}{d \log a}, \quad (1)$$

where a is cosmic expansion factor and $D_+(a)$ is the linear growth rate of density perturbations. The quantity $f(a)$ is well approximated

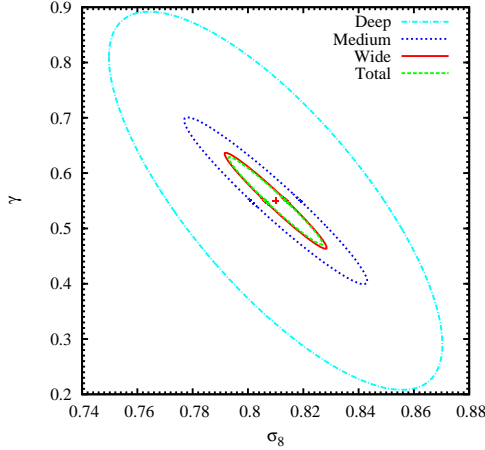


Fig. 6. Constraints on the power-spectrum normalization σ_8 , and on the growth index γ from the three WFXT surveys and from their combination.

by the phenomenological relation (e.g. Wang & Steinhardt 1998)

$$f(a) \simeq \Omega_m(a)^\gamma \quad (2)$$

with $\gamma = 0.55 + 0.05[1 + w(a = 0.5)]$ for large classes of DE models (e.g. Linder 2005). Therefore, testing the precision with which γ can be measured should be regarded as a test of the precision with which General Relativity (GR) can be verified on cosmological scales. For instance, $\gamma \simeq 0.68$ corresponds to the linear growth predicted by the popular DGP model of modified gravity (Dvali et al. 2000).

In order to test the constraints on the growth of perturbations obtainable from the WFXT surveys, we freeze cosmic expansion to Λ CDM, under the assumption that any modified gravity model should be almost indistinguishable from Λ CDM at the background level. Furthermore, we do not include any Dark Energy in our non-GR models, following the idea that a modification of GR should be alternative to DE to explain cosmic expansion. The results of our analysis based on the WFXT surveys are shown in Figure 6. Here we report the expected constraints on the γ - σ_8 plane, once we marginalize over the remaining parameters. This plot confirms that WFXT would indeed

provide very useful constraints on possible deviations from the standard gravity, based on the growth of structure as traced by the evolution of the cluster population.

4. Synergies & legacy value

Addressing the outstanding questions outlined above will greatly benefit from a coordinated multi-wavelength activity between WFXT, future space missions and ground-based facilities (see also Rosati et al. in this volume, for a more detailed description of the synergies between WFXT and future instrumentation).

The identification and characterization of the galaxy populations hosted by the $\sim 2 \times 10^5$ clusters at $z > 0.5$, unveiled by WFXT, will be an essential process to obtain a comprehensive and self-consistent picture of the cosmic cycle of baryons in their hot and cold phase, by tracing the evolution of their underlying stellar populations and star formation histories. Deep optical coverage of large survey areas will be provided by the next generation of wide-field ground-based facilities, currently under development and scheduled for routine operations within the next few years, such as Pan-Starrs³ and LSST⁴.

The combination of WFXT with the ESA Euclid and the NASA JDEM missions, currently under development (Euclid and JDEM) will provide spectroscopic confirmation for a large fraction of $z > 0.5$ clusters identified by WFXT and a full characterization of member galaxies with high resolution optical imaging. Such Dark Energy missions are also designed to reconstruct the DM mass distribution via weak lensing tomographic techniques. This will allow direct lensing mass determination of thousands of massive clusters out to $z \sim 1$. Their comparison with X-ray derived masses will yield the much heralded cluster mass calibration and control of systematics for cosmological applications.

The Atacama Cosmology Telescope (ACT) and the South Pole Telescope (SPT) have recently opened a new era

³ <http://pan-starrs.ifa.hawaii.edu/>

⁴ <http://www.lsst.org/>

of Sunyaev-Zeldovich (SZ) cluster search (Staniszewski & et al. 2009). Next generation large single-dish mm telescopes, such as the Caltech-Cornell Atacama Telescope (CCAT <http://www.submm.org/>) will have enough sensitivity and angular resolution to carry out large-area SZ surveys, providing at the same time spatially resolved SZ imaging for moderately distant massive clusters. Taking advantage of the different dependence of the SZ and X-ray signals on gas density and temperature, their combination will provide a reconstruction of temperature and mass profiles, independent of X-ray spectroscopy (e.g. Ameglio et al. 2009; Golwala et al. 2009). This will offer further independent means of calibrating mass measurements of clusters.

With its unprecedented grasp and angular resolution, WFXT will be an outstanding source of interesting targets for follow-up studies of galaxy clusters with facilities such as JWST, ALMA, ELT and future X-ray observatories (i.e., IXO and Gen-X). For example, a combined study of X-ray luminous proto-cluster regions with ALMA, will test whether a phase of vigorous star formation (sub-mm bright galaxies) coexist with a BH accretion phase. Follow-up pointed observations with IXO of extreme clusters identified by WFXT at $z \sim 2$ will allow the study of metallicity and entropy structure of the pristine ICM. In general, the synergy with next generation multi-wavelength deep wide-area surveys and with high sensitivity instruments for pointed observations will unleash the full potential of WFXT in addressing a number of outstanding scientific questions related to cosmological and astrophysical applications of galaxy clusters.

Acknowledgements. This work has been supported by ASI-AAE Grant for Mission Feasibility Studies and by the INFN PD51 grant. The Authors would like to thank all the members of the WFXT team for a number of enlightening discussions.

References

- Albrecht, A., Amendola, L., Bernstein, G., et al. 2009, ArXiv e-prints, 0901.0721
- Ameglio, S., Borgani, S., Pierpaoli, E., et al. 2009, MNRAS, 394, 479
- Balestra, I., Tozzi, P., Ettori, S., et al. 2007, A&A, 462, 429
- Baumgartner, W. H., Loewenstein, M., Horner, D. J., & Mushotzky, R. F. 2005, ApJ, 620, 680
- Borgani, S., Governato, F., Wadsley, J., et al. 2002, MNRAS, 336, 409
- Borgani, S. & Kravtsov, A. 2009, ArXiv e-prints
- Borgani, S., Rosati, P., Tozzi, P., et al. 2001, ApJ, 561, 13
- Borgani, S. & Viel, M. 2009, MNRAS, 392, L26
- Burns, J. O., Hallman, E. J., Gantner, B., Motl, P. M., & Norman, M. L. 2008, ApJ, 675, 1125
- Carilli, C. L., Harris, D. E., Pentericci, L., et al. 2002, ApJ, 567, 781
- Cunha, C., Huterer, D., & Dore, O. 2010, ArXiv e-prints
- Desjacques, V. & Seljak, U. 2010, ArXiv e-prints
- Donahue, M., Horner, D. J., Cavagnolo, K. W., & Voit, G. M. 2006, ApJ, 643, 730
- Dvali, G., Gabadadze, G., & Porrati, M. 2000, Physics Letters B, 485, 208
- Fabian, A. C. 1994, ARA&A, 32, 277
- Giacconi, R., Borgani, S., Rosati, P., et al. 2009, in Astronomy, Vol. 2010, Astro2010: The Astronomy and Astrophysics Decadal Survey, 90
- Golwala, S. R., Aguirre, J. E., Basu, K., et al. 2009, in Astronomy, Vol. 2010, astro2010: The Astronomy and Astrophysics Decadal Survey, 96–+
- Haiman, Z., Mohr, J. J., & Holder, G. P. 2001, ApJ, 553, 545
- Hatch, N. A., Overzier, R. A., Kurk, J. D., et al. 2009, MNRAS, 395, 114
- Komatsu, E., Smith, K. M., Dunkley, J., et al. 2010, ArXiv e-prints, 1001.4538
- Kravtsov, A. V., Vikhlinin, A., & Nagai, D. 2006, ApJ, 650, 128
- Lau, E. T., Kravtsov, A. V., & Nagai, D. 2009, ApJ, 705, 1129
- Leccardi, A. & Molendi, S. 2008a, A&A, 487, 461
- Leccardi, A. & Molendi, S. 2008b, A&A, 486, 359

- Lima, M. & Hu, W. 2004, *Phys. Rev. D*, 70, 043504
- Linder, E. V. 2005, *Phys. Rev. D*, 72, 043529
- Majumdar, S. & Mohr, J. J. 2003, *ApJ*, 585, 603
- Mantz, A., Allen, S. W., Rapetti, D., & Ebeling, H. 2009, ArXiv e-prints, 0909.3098
- Maughan, B. J. 2007, *ApJ*, 668, 772
- Maughan, B. J., Jones, C., Forman, W., & Van Speybroeck, L. 2008, *ApJS*, 174, 117
- McNamara, B. R. & Nulsen, P. E. J. 2007, *ARA&A*, 45, 117
- Miley, G. K., Overzier, R. A., Zirm, A. W., et al. 2006, *ApJ*, 650, L29
- Mushotzky, R. F. 2004, in *Clusters of Galaxies: Probes of Cosmological Structure and Galaxy Evolution*, ed. J. S. Mulchaey, A. Dressler, & A. Oemler, 123–+
- Oguri, M. 2009, *Physical Review Letters*, 102, 211301
- Peterson, J. R. & Fabian, A. C. 2006, *Phys. Rep.*, 427, 1
- Piffaretti, R. & Valdarnini, R. 2008, *A&A*, 491, 71
- Pratt, G. W., Arnaud, M., Piffaretti, R., et al. 2009, ArXiv e-prints, 0909.3776
- Pratt, G. W., Böhringer, H., Croston, J. H., et al. 2007, *A&A*, 461, 71
- Rasia, E., Ettori, S., Moscardini, L., et al. 2006, *MNRAS*, 369, 2013
- Rassat, A., Amara, A., Amendola, L., et al. 2008, ArXiv e-prints, 0810.0003
- Rosati, P., Borgani, S., & Norman, C. 2002, *ARA&A*, 40, 539
- Santos, J. S., Rosati, P., Tozzi, P., et al. 2008, *A&A*, 483, 35
- Saro, A., Borgani, S., Tornatore, L., et al. 2009, *MNRAS*, 392, 795
- Sartoris, B., Borgani, S., Fedeli, C., et al. 2010, ArXiv e-prints
- Schindler, S. & Diaferio, A. 2008, *Space Science Reviews*, 134, 363
- Shang, C., Crotts, A., & Haiman, Z. 2007, *ApJ*, 671, 136
- Snowden, S. L., Mushotzky, R. F., Kuntz, K. D., & Davis, D. S. 2008, *A&A*, 478, 615
- Staniszewski, Z. & et al. 2009, *ApJ*, 701, 32
- Sun, M., Voit, G. M., Donahue, M., et al. 2009, *ApJ*, 693, 1142
- Tozzi, P. & Norman, C. 2001, *ApJ*, 546, 63
- Verde, L. 2010, ArXiv e-prints, 1001.5217
- Vikhlinin, A., Kravtsov, A. V., Burenin, R. A., et al. 2009a, *ApJ*, 692, 1060
- Vikhlinin, A., Markevitch, M., Murray, S. S., et al. 2005, *ApJ*, 628, 655
- Vikhlinin, A., Murray, S., Gilli, R., et al. 2009b, in *Astronomy*, Vol. 2010, *Astro2010: The Astronomy and Astrophysics Decadal Survey*, 305
- Voges, W., Aschenbach, B., Boller, T., et al. 1999, *A&A*, 349, 389
- Voit, G. M. 2005, *Reviews of Modern Physics*, 77, 207
- Voit, G. M., Balogh, M. L., Bower, R. G., Lacey, C. G., & Bryan, G. L. 2003, *ApJ*, 593, 272
- Wang, L. & Steinhardt, P. J. 1998, *ApJ*, 508, 483
- Werner, N., de Plaa, J., Kaastra, J. S., et al. 2006, *A&A*, 449, 475